Journal of Advanced College of Engineering and Management, Vol. 9, 2024

SIMULATION FOR SAND EROSION IN KAPLAN RUNNER BLADE: A CASE STUDY OF GANDAK HYDRO POWER STATION

Anil Shah[1,*], Raj Kumar Chaulagain[2]

[1] *"Department of Automobile and Mechanical Engineering, Thapathali Campus, IOE, Tribhuvan University, Nepal"*

***[1]Email**: anyl.shah777@gmail.com

Abstract

Gandak Hydropower station (GHPS) is located at Nawalparasi of total capacity 15 MW with adjustable blade bulb/tubular turbine with three units of each 5 MW. Huge sand concentration especially during monsoon and over 40 years of operation, turbine components at GHPS are severely eroded. This study aimed to detect the erosion prone section of Kaplan runner blade by CFD analysis using ANSYS Fluent and comparing qualitatively with eroded runner blade of GHPS. Sand analysis as per site conditions was performed in lab for mineral content, particle size distribution and sediment concentration. It can be concluded from the results of CFD simulations, mostly upper portion of blade region is affected by sediment erosion. In upper portion, trailing edges are more densely affected than leading edges. Erosion rate density increases with increase in sediment particle size and sediment concentration. Comparing qualitatively of eroded Kaplan runner blade at GHPS and CFD simulation results, erosion most affected zone of Kaplan runner blade is found to be similar. To increase life of runner blade from effects of sand erosion, upper portion of blade surface should be frequently observed and protected by suitable coatings.

Keywords: *Sand Erosion – Computational Fluid Dynamics (CFD) –Kaplan Runner Blade- Bulb Turbine– Discrete Phase Modeling*

1. INTRODUCTION

Sand erosion is unavoidable phenomenon in the operation of hydraulic turbines. Due to sand erosion, turbine components can be damaged and also loss in efficiency with requirement of frequent maintenance can occur. The Kaplan turbine is an axial flow turbine and falls under category of reaction type turbine which is used for low head and high discharges hydropower plants. Bulb turbine is reaction turbine of Kaplan type which consists essential turbine components as well as the generator inside a bulb with absence of spiral casing. Bulb or Tubular turbine is quite suitable for heads varying from 3 m to 15m, better efficiency due to straight flow passage and at part load there is reduced loss of efficiency (Rajput, 2016). Figure 1 shows schematic diagram of bulb turbine.

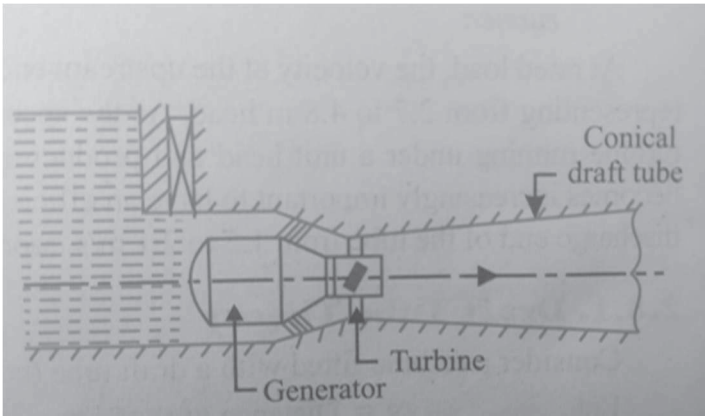

Figure 1: Bulb turbine layout (Rajput, 2016)

Gandak Hydropower Station is situated at Pratappur Gaunpalika, District: Nawalparasi, Nepal The plant has adjustable blade tubular (Kaplan) horizontal mounted turbines with three units of 5 MW each having aggregate capacity of 15 MW. The salient features of GHPS include discharge with 103 .84 m^3/s and gross head gross head/Net head=7.59 m/6.09 m , turbine speed 107 rpm. (NEA Generation Magazine, 2023). Figure 2 shows turbine overview of Gandak Hydropower Station.

In a case study of erosion in Kaplan turbine by measurements of eroded portions for two years, a standard erosion model was applied to estimate the erosion in Kaplan turbine blade, runner chamber and draft tube cone. The study showed that the trailing side of the turbine blade is most prone to erosion whereas furrows of erosion are caused in tip side (RAI & KUMAR, 2016). Research was conducted on cavitation characteristics of Kaplan turbine under sediment flow conditions by using CFD mode. The more the sediment concentration and the large the sand diameter, the serious the runner is abraded, and the greater the efficiency is decreased (Weili et al., 2010).

CFD analysis performed to evaluate the efficiency of Kaplan turbine under different silt parameters and the result showed that the regions around trailing edge found to be more affected due to silt erosion (Sangal et al., 2016). The study showed that mineral content, size, shape and texture are the most important parameters of sand. It was depicted that greater the size greater is the impact on hydraulic turbine(Poudel et al., 2012).

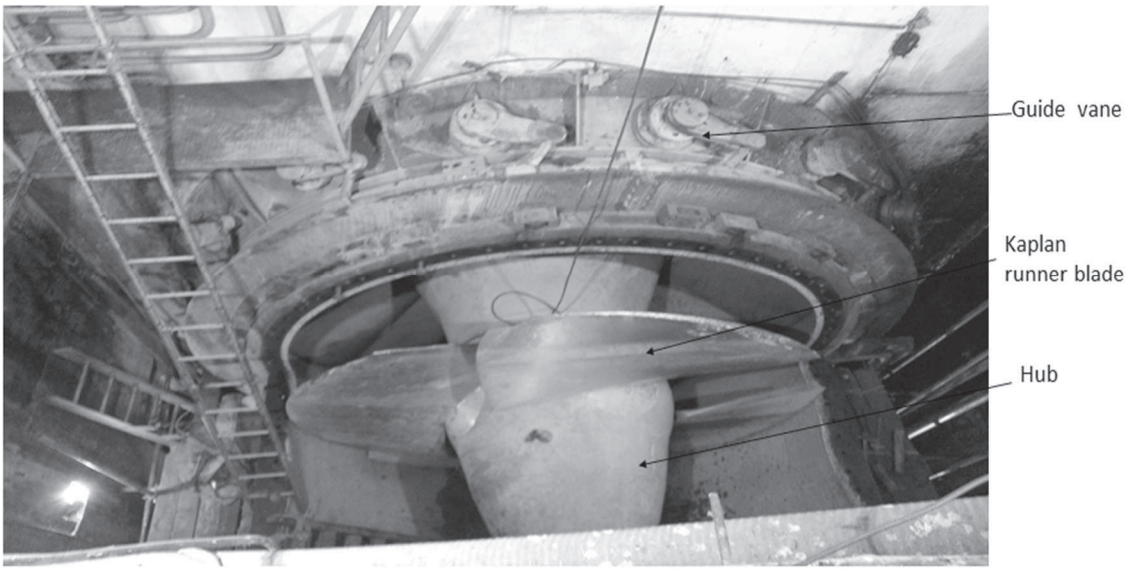

Figure 2: Bulb Turbine at Gandak Hydropower Station (site visit)

A series of excellent Kaplan turbine models were selected, and numerical calculation within whole flow passage was carried out by CFD simulation. and found the hydraulic loss in spiral case was smaller than that in guide vane and the draft tube (Li & Liu, 2020). Sediment content of water can no more be overlooked in any phase of hydropower project implementation, design, operation and maintenance, and refurbishment and upgrading. One solution in order to decrease the sediment erosion is to increase the size of the turbine, thereby increases the hydraulic radius of curvature, and thus decreases the accelerations (Hari Prasad Neopane et al., 2011).

The studied showed average sediment concentration in discharged water of triveni and illustrate the

channel planform of the Gandak River in the plain (Prasad & Rishideo, 2021). The erosion of hydraulic machinery depends on eroding particles, that is, their size, shape and hardness; on substrates, their chemistry, elastic properties, surface hardness and surface morphology; and on operating conditions, velocity, impingement angle and concentration (Thapa et al., 2005). Figure 4 shows Quartz content trom mineral analysis of different rivers of Nepal and erosion rate density from corresponding sand samples.

Low head Kaplan blade tips and region around trailing edge are highly exposed to sand erosion. Erosion damage may be reduced by making straight surfaces toward trailing edges (Thapa, 2004). Erosion was observed in nozzle of the Pelton turbines due to sand particles in 22MW Chilime Hydropower Plant in Nepal. High quartz content and increase sediment load during monsoon along with the small particle size are the major cause for the severe erosion of turbine parts, namely the nozzle and buckets (Bajracharya et al., 2008).

In the study of fluid flow analysis in enhanced Kaplan turbine by changing the blade design using ANSYS software, the more energy was consumed even at low pressure of water flow in the turbine (Gupta et al., 2017). A bulb turbine, without the conventional guide vanes, has been designed and numerically investigated which show hydraulic efficiency of the turbine is slightly lower due to increase in losses at the draft tube section and recommended further studies to minimize the losses in the draft tube (Shandilya et al., 2019).

The highest velocities and accelerations occurred at outlet of the runner blade and more erosion was predicted especially at the pressure side of the blade outlet and at the shroud in the study of sediment erosion analysis of a Francis turbine and also concluded that if the particle size in the water increases beyond critical particle sizes, the turbine should not be operated at low guide vane opening(Neopane, 2010). The synergic effect of sand erosion and cavitation is more pronounced than their individual effects in the hydraulic turbine components (Thapa et al., 2007).

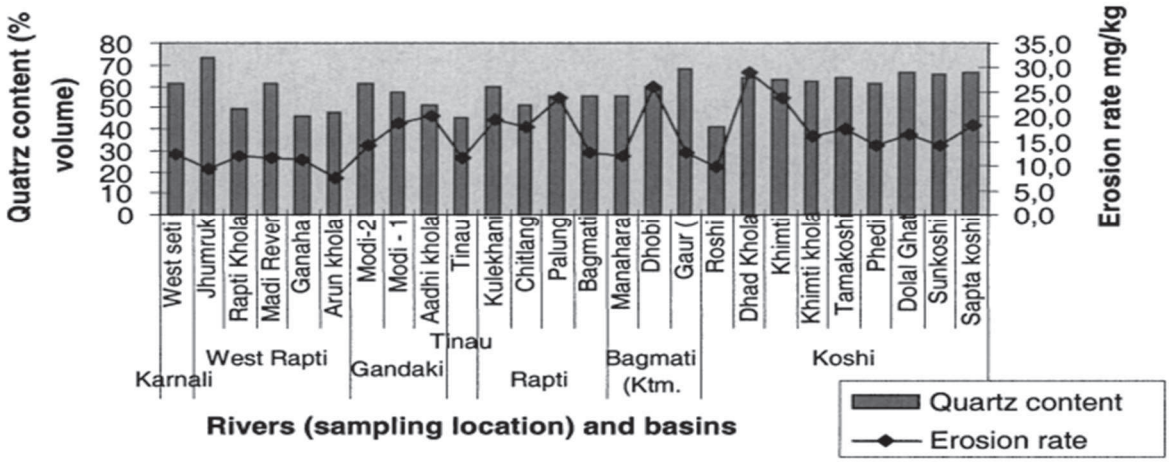

(Thapa et al., 2005)

Figure 4: Quartz content and erosion rate density from corresponding sand samples

Huge sand concentration and over 40 years of operation, turbine components at GHPS are severely eroded and efficiency is reduced. There is still research gap in the field of study of erosion behavior due to sand on Kaplan turbine blade using simulation software and comparing the results with similar

hydroelectric power plants. The objective of the research is to study about sand erosion pattern on Kaplan turbine blade by CFD analysis under various silt operating conditions and parameter. The eroded analysis is assumed to performed in Kaplan turbine blade only neglecting other effects like cavitation. During field visit, erosion affected zone of runner blade was observed at GHPS as shown in Figure 3. It was noticed that thickness of runner blade have been eroded significantly affecting more at upper portion of blade with dense effects towards trailing side than leading side.

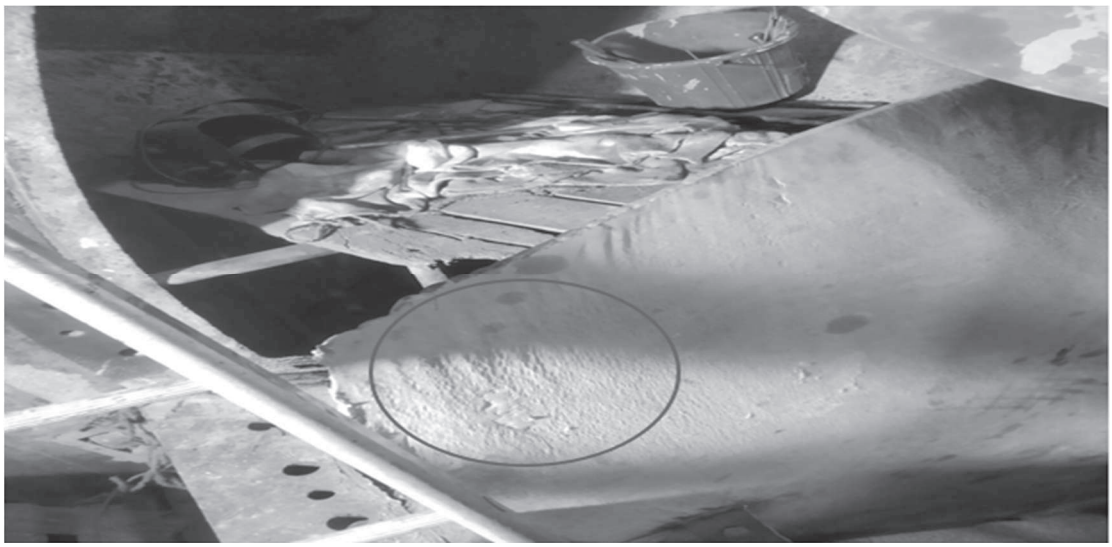

Figure 3: Erosion on Kaplan runner blade at GHPS

2. METHODOLOGY

Previous background of sand erosion on Kaplan turbine have been referred from available books, journals, conference papers & websites. 3D Geometic model of the Kaplan turbine blade have been generated using SolidWorks 2021 software as per parameters available from case study area i.e GHPS by field visit. Figure 5 shows 3D model of runner blade, Figure 6 shows assembled components and Figure 7 shows complete geometry of model with casing using Soliworks,. The generated model have been imported into simulation software ANSYS Fluent 2023R1 and suitable meshing by division of the flow domain into discrete control volumes using a computational grid generator ANSYS meshing have been done. CFD simulations have been carried out for different silting conditions and concentration applying suitable boundary conditions. Comparison of simulations output with case study area of hydroelectric power plant have been done qualitatively. Results for velocity, pressure and erosion contours under different operating parameters for sand erosion related issue have been obtained after simulations and analyzed for sand erosion pattern on Kaplan turbine blade.

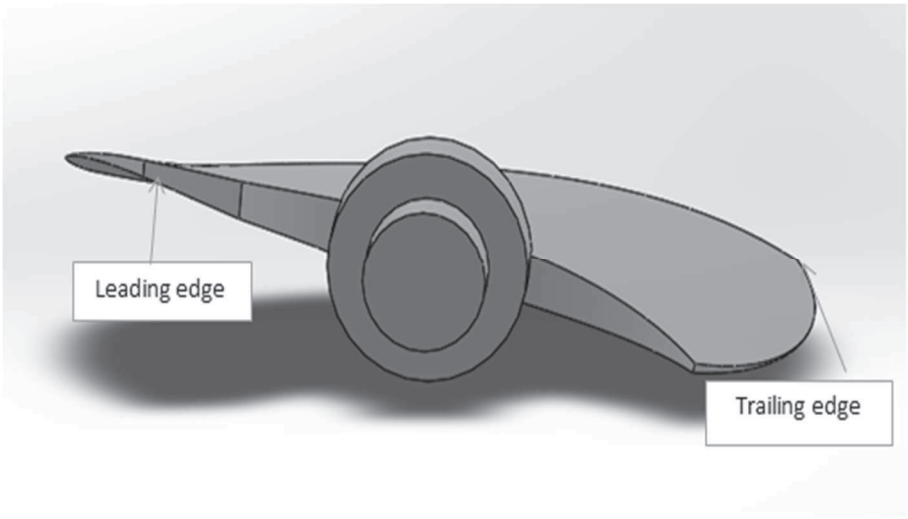

Figure 5: Runner blade front view (3D model) using SolidWorks

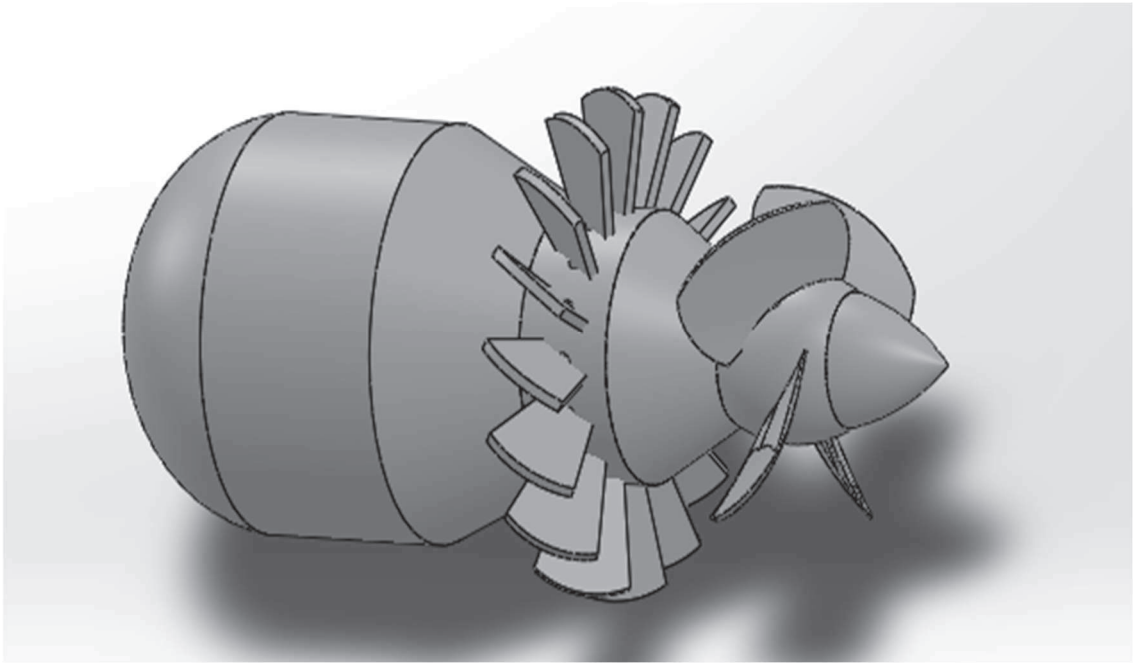

Figure 6:Assembled turbine components using SolidWorks

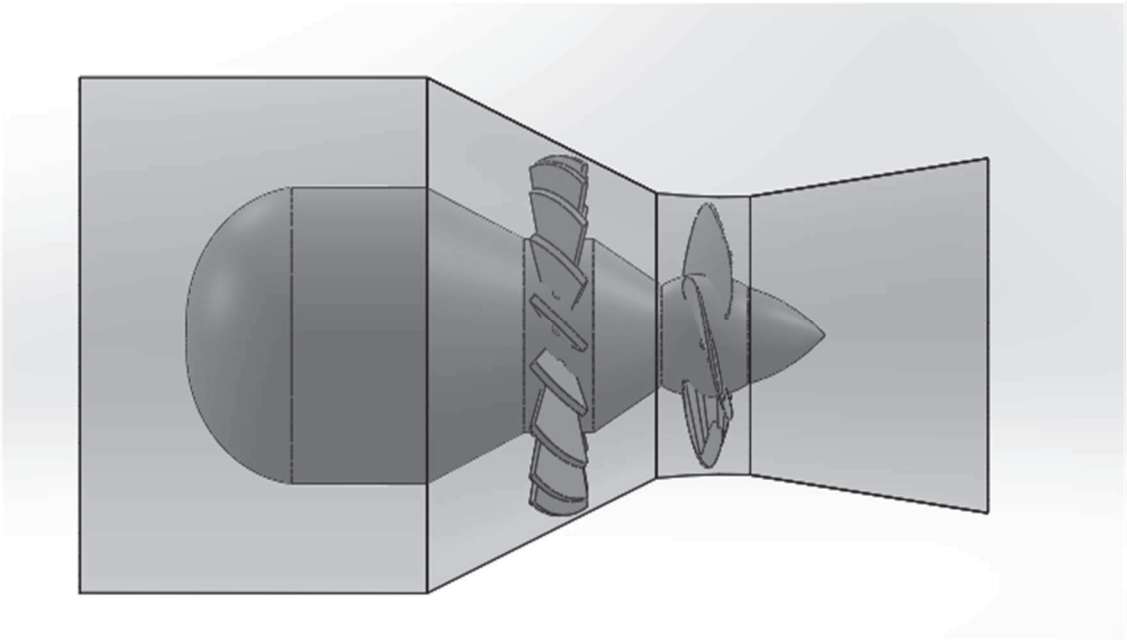

Figure 7: Complete Geomtery for CFD analysis

3. SIMULATION

Computational Fluid Dynamics (CFD) is one of the branches of fluid mechanics that uses numerical methods and algorithms to solve and analyze problems that involve fluid flows. CFD codes are structured around the numerical algorithms that can tackle fluid flow problems (Versteeg & Malalasekera, 2007). The CFD code Fluent was used for solving this problem. The system of governing equations was solved by control volume approach which converts the governing equations to a set of algebraic equations that can be solved numerically. The control volume approach employs the conservation statement or physical law represented by the entire governing equations over finite control volumes. Grid schemes used are staggered in which velocity components are evaluated at the center of control volume interfaces and all scalar quantities are evaluated in the center of control volume. The analysis is carried out from bulb to draft tube, so boundary condition is created as inlet for the location bulb inlet and outlet as draft tube outlet. In the Figure 8, physics setup for analysis is shown as inlet boundary taken as mass flow rate (kg/s), outlet boundary as pressure(Pa) and wall is stationary with no slip between wall and fluid. The mesh for this study was generated by ANSYS Meshing 2023R1 of complete meshed geometry for the CFD analysis as shown in Figure 9. Second order upwind scheme was employed to discretize equations. Pressure and velocity were coupled. In all cases, the residual terms for all of the equations were less than 10^{-6}. Discrete Phase Model (DPM) set up was used to inject silt particles enabling to compute the trajectories of particles based on various silt size and concentration as per site conditions. The turbulence model is set as Shear Stress Transport (SST). The analysis followed is transient type.

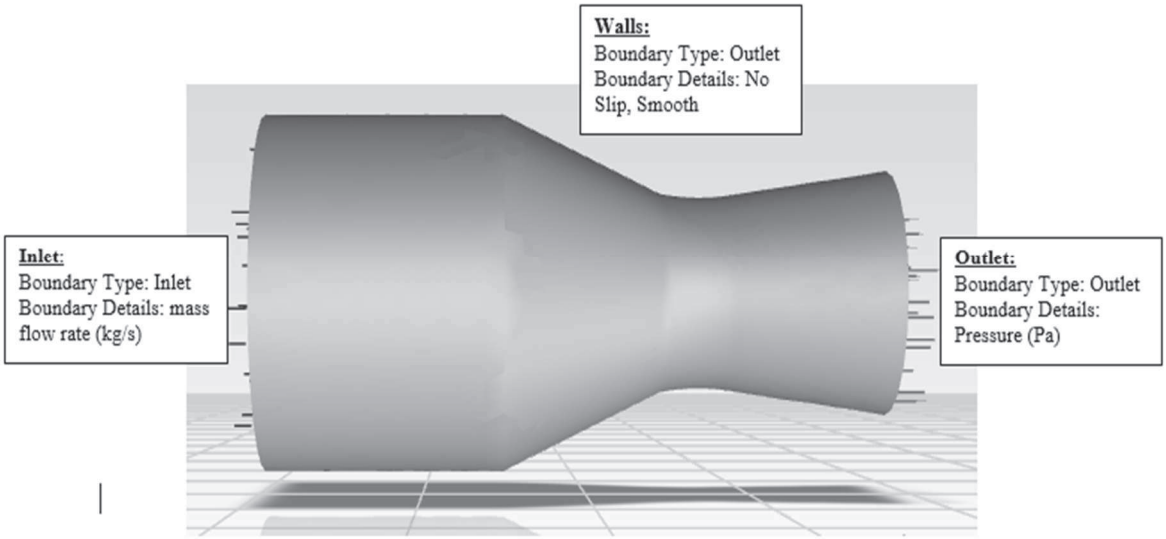

Figure 8: Physics setup

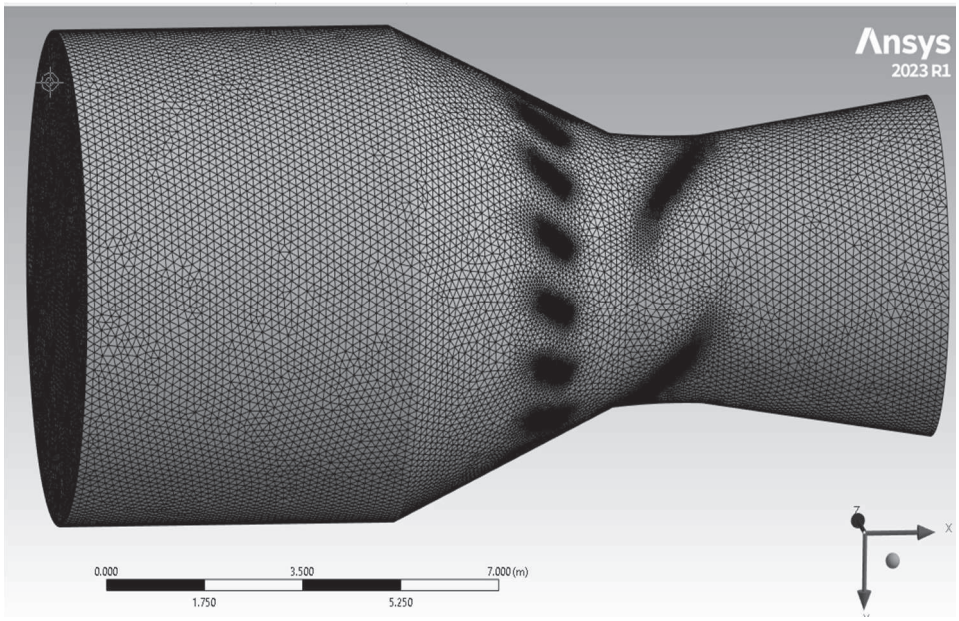

Figure 9: Complete meshed geometry

- **Flow Calculations**

Power input, power output, and efficiency were then calculated using equations given below.

Power, P = ρgQH *Equation 1*

Where,

ρ = water density =1000 kg/m^3

g = gravitational acceleration=9.81 m/s^2

Q = discharge

H=head

Discharge

$Q = \frac{\pi}{4} * (D_{run}^2 - D_{hub}^2) * V_f \quad m^3/s$ *Equation 2* (Rajput, 2016)

Where,

D_{run} = diameter of runner

D_{hub} = diameter of hub

V_f = velocity of flow

Specific speed $N_s = \frac{N\sqrt{P}}{H^{5/4}}$ *Equation 3* (Rajput, 2016)

Where,

N= speed of turbine

H = head

P = power

4. RESULTS AND DISCUSSIONS

Various CFD simulation carried out to predict erosion distribution over runner blade. As higher computer configuration was required for full (actual) scale geometry simulations, so reducing scale 1:10 was used for the research.

4.1 Mesh Independence test

In order to ensure that the calculated results are grid independent, eight different tetrahedral grid distributions were tested for their performance to predict the torque as shown in Figure 10. In the figure, it was observed that torque slightly increased and finally becomes constant beyond a certain number of mesh elements. Beyond this, any further increase in the number of mesh elements only increased the computational time, without any significant improvement in torque accuracy. So, optimum 1580000 cells or elements was selected for further study. The time for completion of simulation result takes nearly 10 hours.

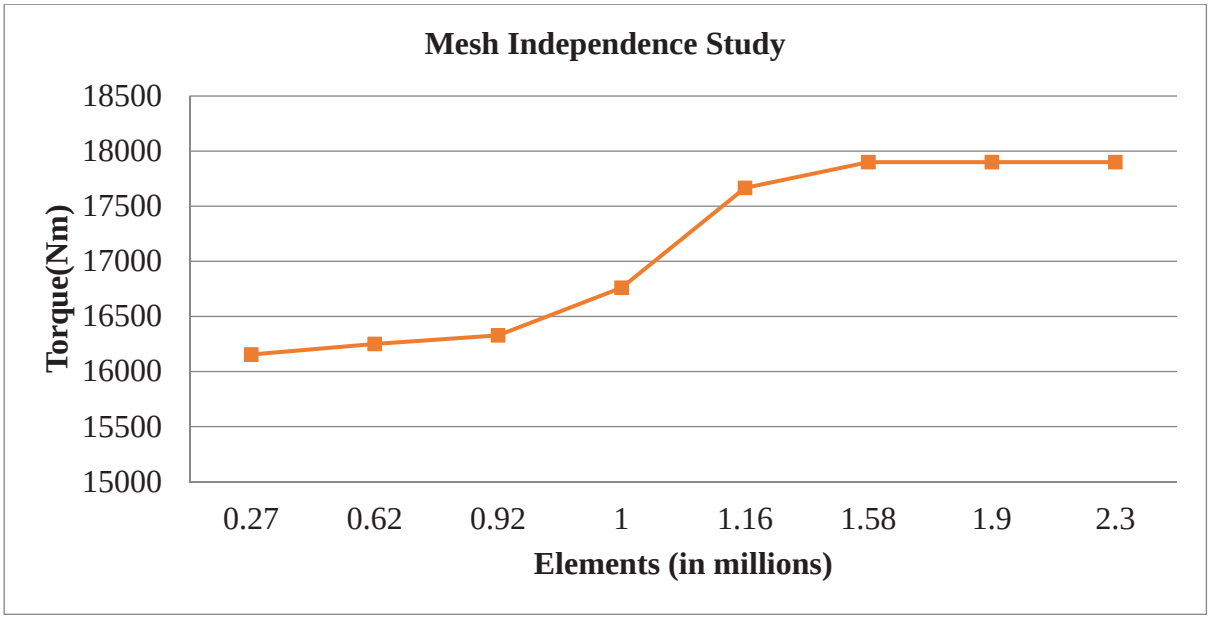

Figure 10: Optimum grid size

4.2 Velocity Contour

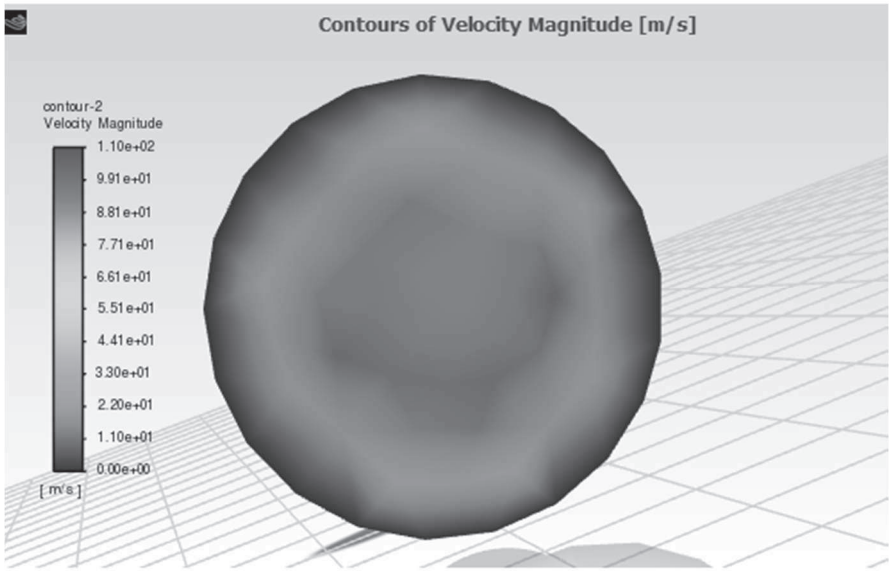

Figure 11: Velocity outlet of runner

(silt concentration 13096 ppm, silt size 0.5 mm)

From the Figure 11, it can be shown that the velocity are unevenly distributed which can suggest high turbulence

4.3 Pressure Contour

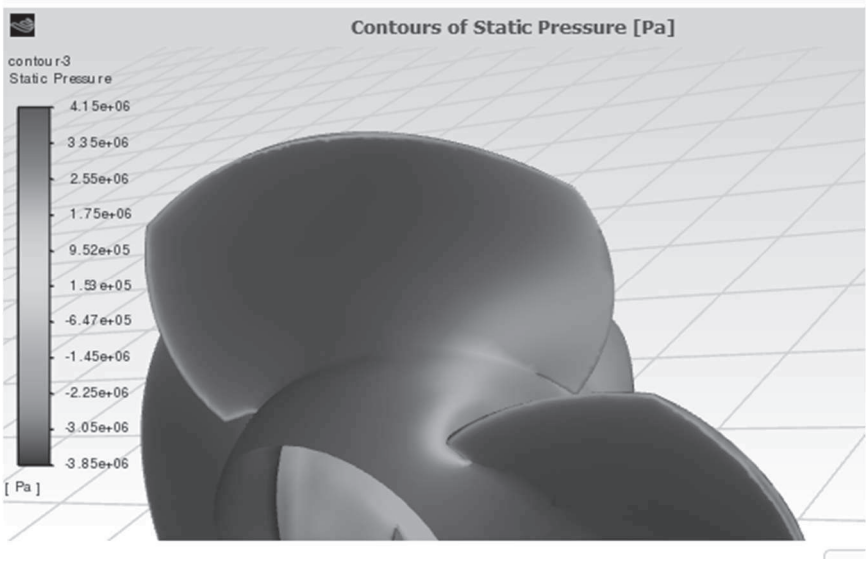

Figure 12: Pressure contour on pressure side

(silt concentration 13096 ppm, silt size 0.5 mm)

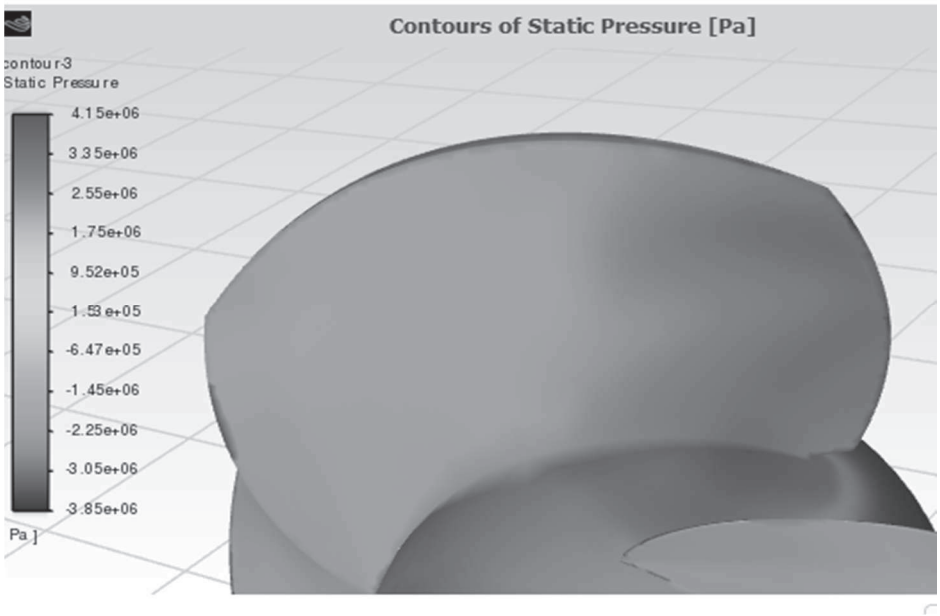

Figure 13: Pressure contour on suction side

(silt concentration 13096 ppm, silt size 0.5 mm)

From the Figure 12, Figure 13 of pressure contour, it was observed that the pressure at the inlet of blade surface was higher and tend to decrease towards the outlet.

4.4 Flow Visualization using Streamlines

A velocity streamline was plotted to visualize water flow streamlines along the geometry as shown in Figure 14.

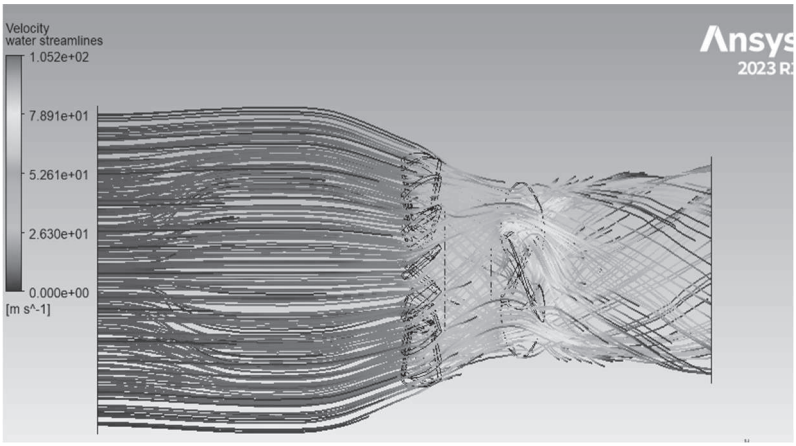

Figure 14: Flow Visualization using streamlines

4.5 Erosion Contour

Various CFD simulations performed to visualize the erosion on the surface of the runner blade and compared with various conditions of silt size, concentration and varying blade angle. Figure 15, Figure 16 shows erosion contour on blade by varying blade angle and indicates trailing side is more affected than leading and other upper section of blade.

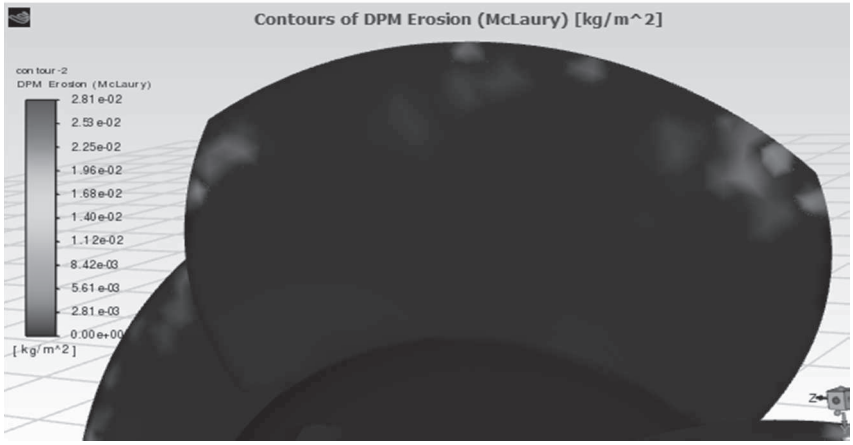

Figure 15: Erosion distribution over blade surface blade angle 80 deg.
(silt concentration 13096 ppm, silt size 0.8 mm)

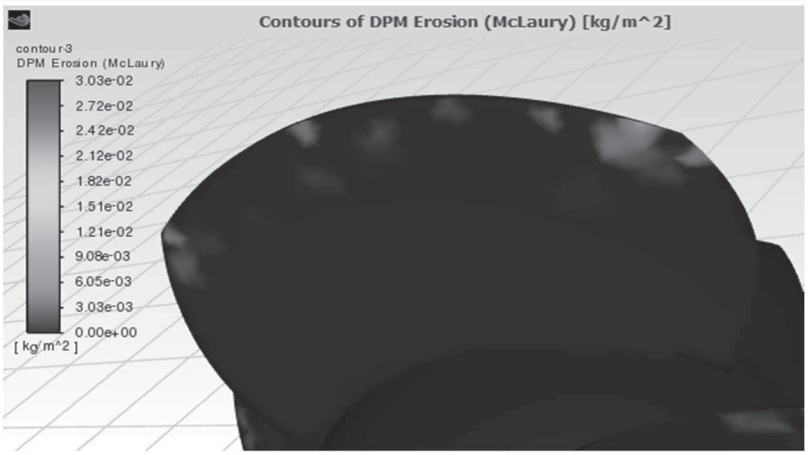

Figure 16: Erosion distribution over blade surface blade angle 50 deg.
(silt concentration 13096 ppm, silt size 0.8 mm)

4.6 Effect Analysis of silt size on erosion

The effect analysis is done by plotting graph of erosion rate over silt size for varying silt conditions. The erosion rate is taken from the CFD simulation. Figure 17, 18 and 19 shows erosion rate density for different silt size 0.5 mm, 0.8 mm and 1 mm operating under same condition of silt concentration and blade angle. Figure 20 shows graph indicating the erosion rate density increases with increase in silt size. So, during monsoon season when silt size increases, the erosion rate density also increases.

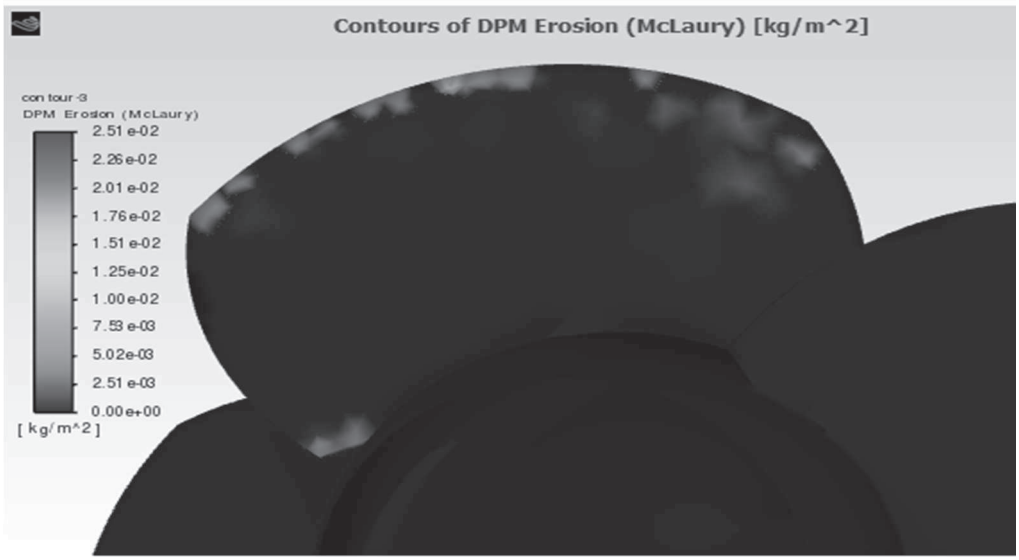

Figure 17: Erosion rate density for silt size 0.5 mm
(silt concentration 13096 ppm, blade angle 80 deg)

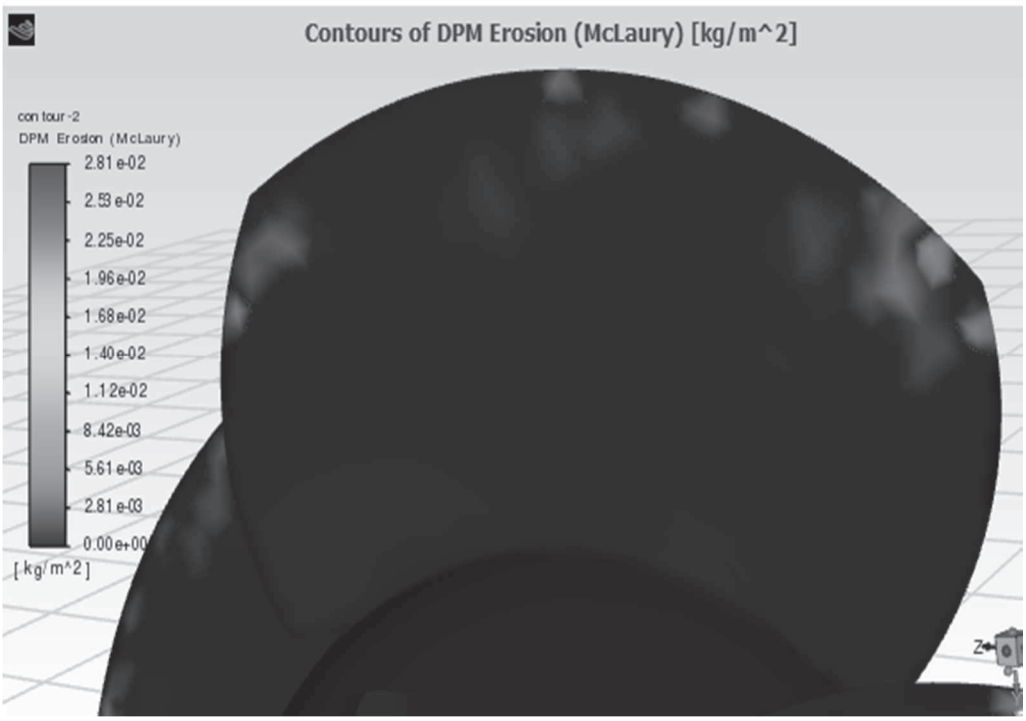

Figure 18: Erosion rate density for silt size 0.8 mm
(silt concentration 13096 ppm, blade angle 80 deg)

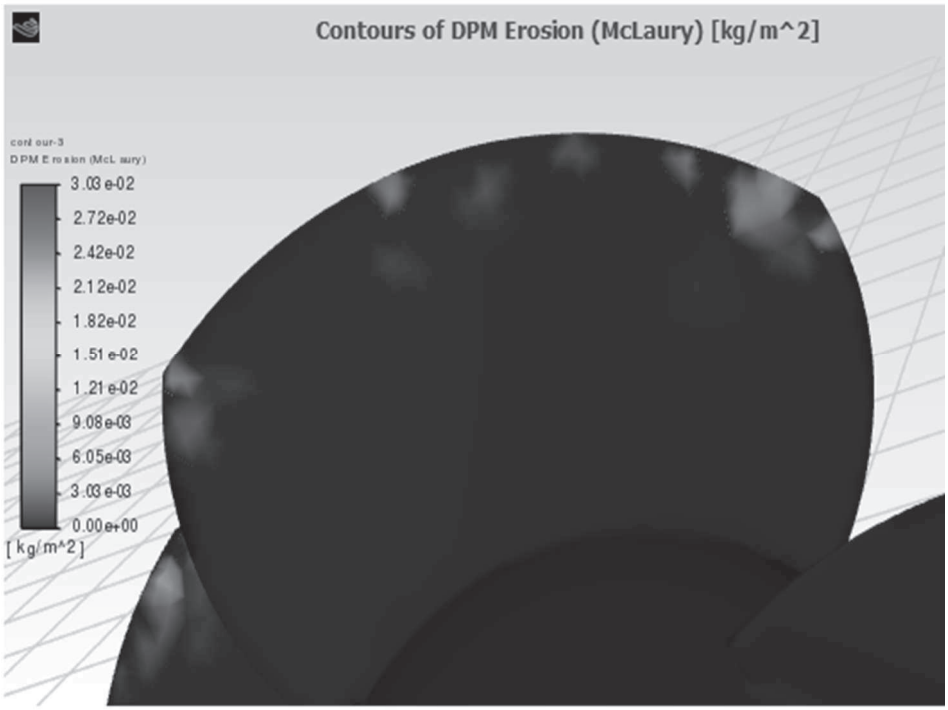

Figure 19: Erosion rate density for silt size 1 mm
(silt concentration 13096 ppm, blade angle 80 deg)

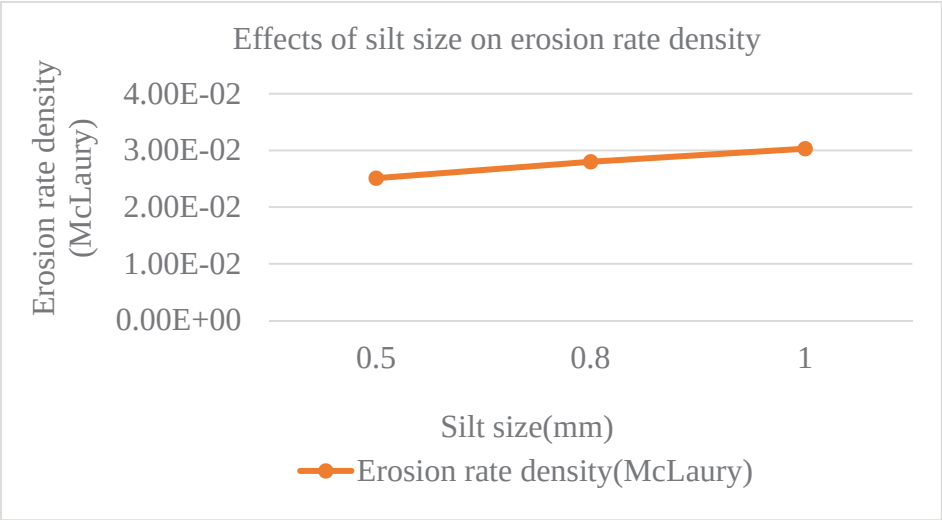

Figure 20: Effects of silt size on erosion rate density

4.7 Effect Analysis of silt concentration on erosion

The effect analysis is done by plotting graph of erosion rate over silt concentration for varying silt conditions. Figure 21, Figure 22 and Figure 23 shows erosion rate density for different silt concentration 4494 ppm, 13096 ppm and 21699 ppm operating under same condition of silt size and blade angle. Figure 24 shows graph which indicates that the erosion rate density increases with increase in silt concentration. Figure 25 shows combination chart of effects of silt size and concentration on erosion rate density indicating erosion rate density increases as silt size and concentration increases.

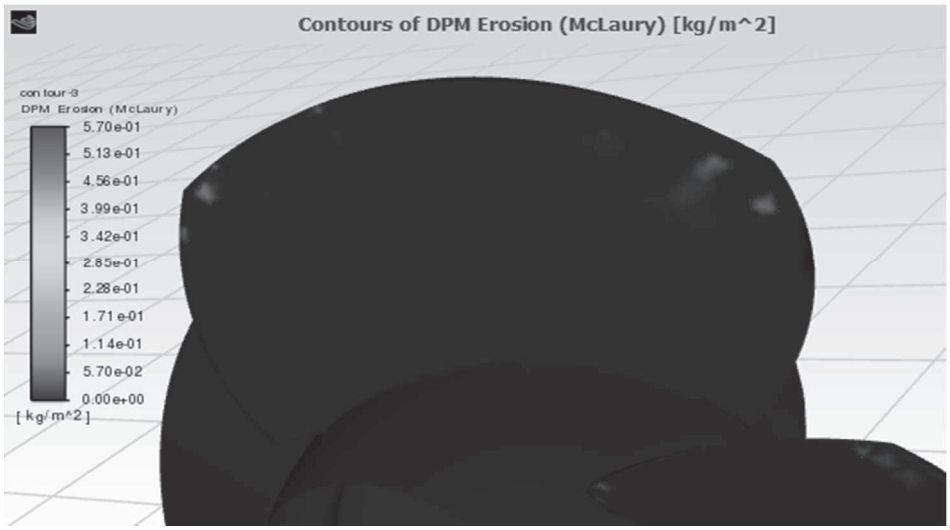

Figure 21: Erosion rate density for silt concentration 4494 ppm

(silt size 0.5 mm, blade angle 80 deg)

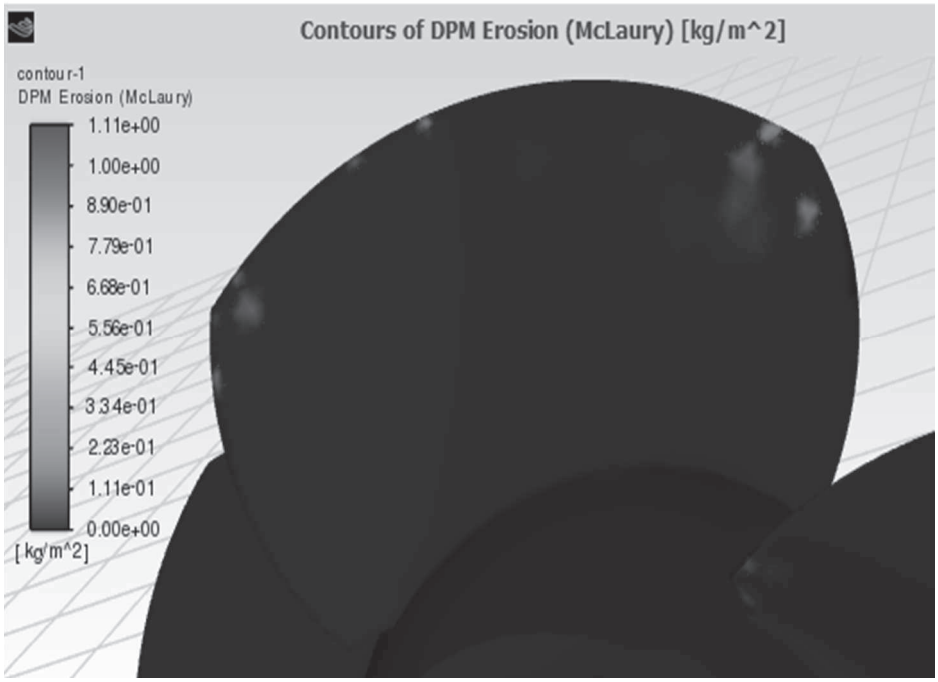

Figure 22: Erosion rate density for silt concentration 13096 ppm

(silt size 0.5 mm, blade angle 80 deg)

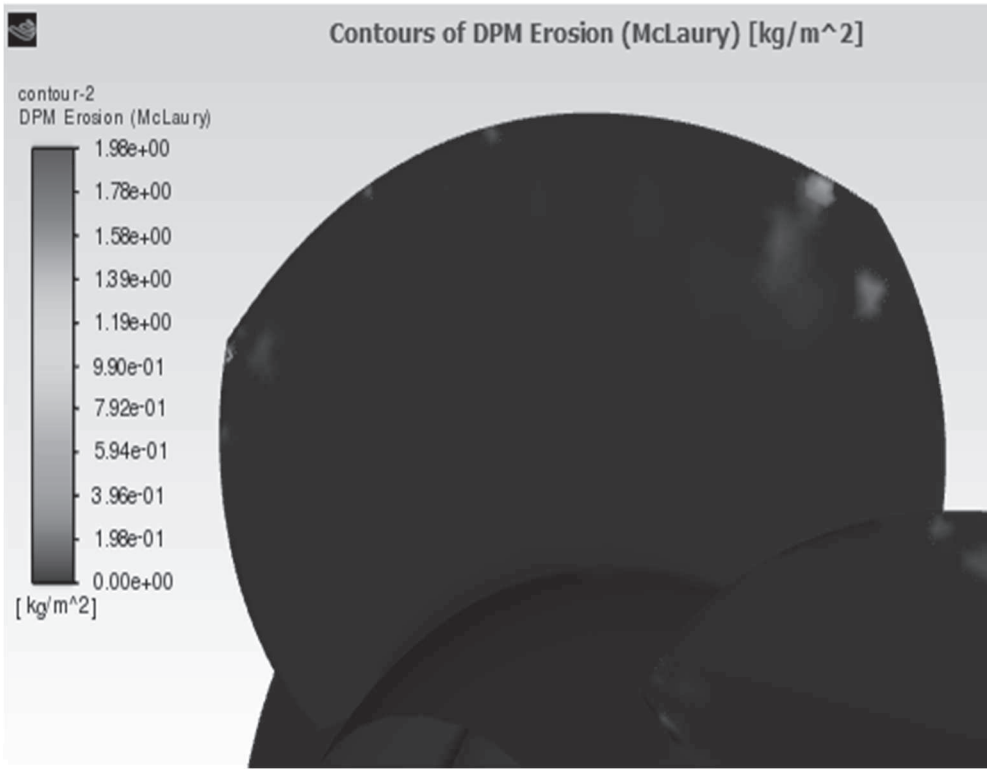

Figure 23: : Erosion rate density for silt concentration 21699 ppm

(silt size 0.5 mm, blade angle 80 deg)

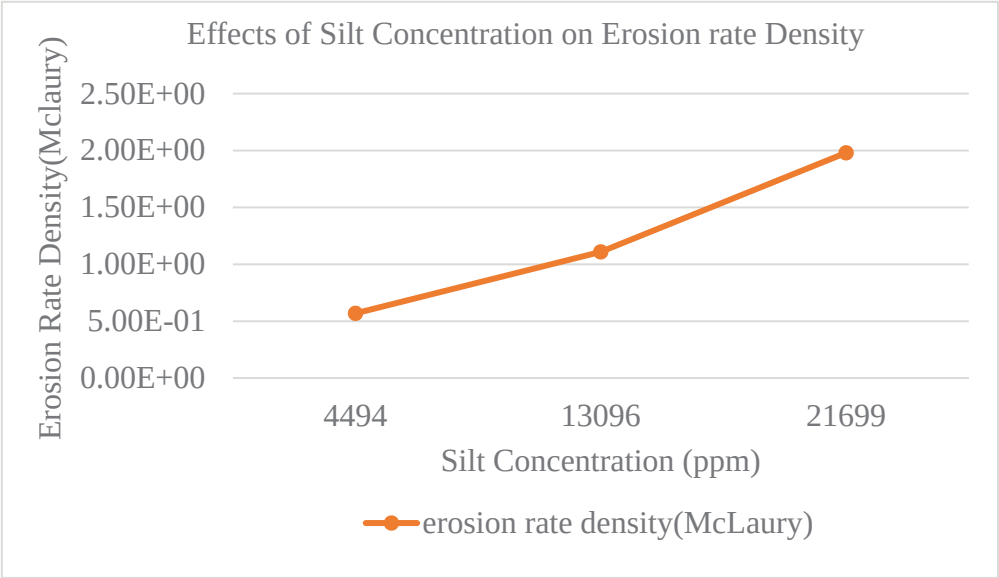

Figure 24: Effects of silt concentration on erosion rate density

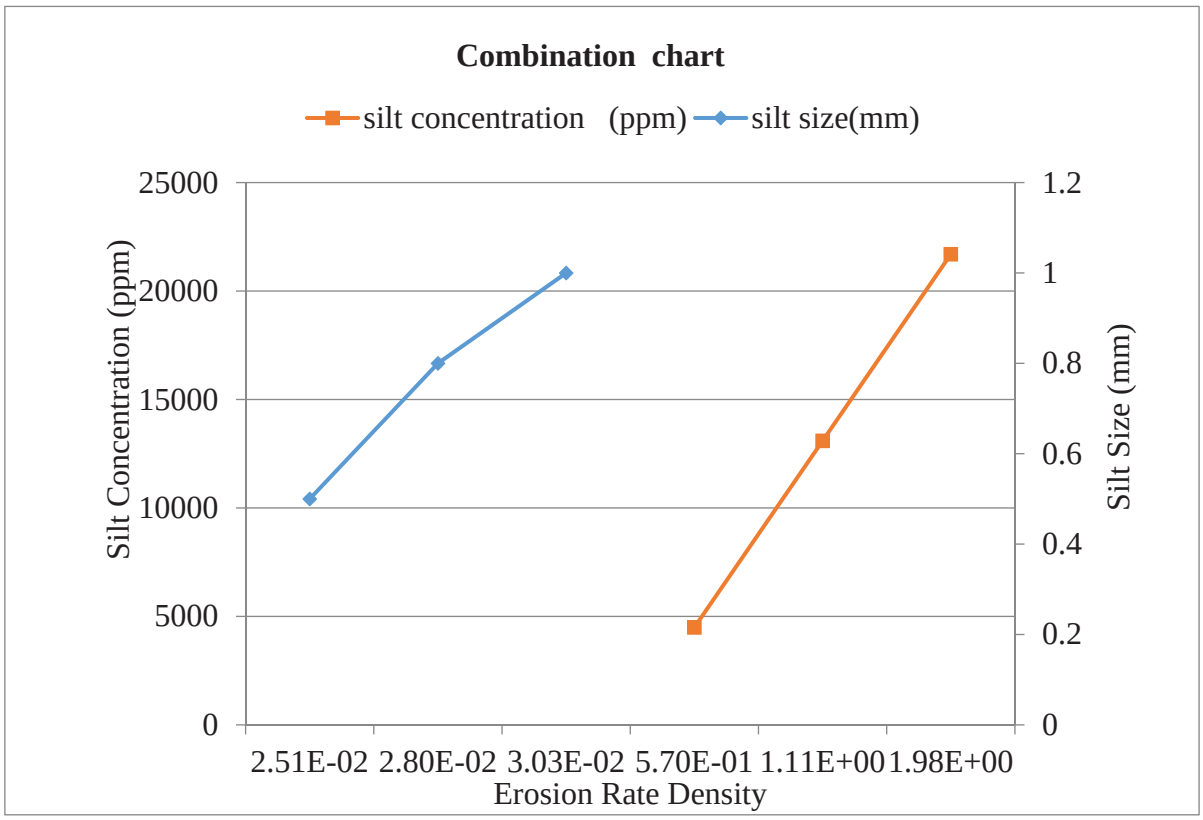

Figure 25: Silt size and concentration Vs erosion rate density

5. CONCLUSION

Erosion due to sand particles on Kaplan runner blade of bulb type turbine have been studied in this research by CFD analysis using geometry of hydroelectric plant Gandak Hydropower Station. It can be concluded that upper portion of Kaplan runner blade is mostly eroded zone from CFD analysis and withstand result with the eroded pattern of site condition i.e. GHPS. In upper portion, trailing edges are more densely affected than leading edges. With the increase in sediment concentration and sand size particles especially during monsoon season, erosion rate density also increases. Low erosion occurs at 80^0 blade opening condition (2.81E-02 kg/m^2s) and erosion increases on 50^0 blade opening (3.03E-02 kg/m^2s).

For more precision analysis, three dimensional (3D) scanning of runner blade and comparision by quantitatively ie. mass loss of blade material is recommended. The thickness observed near the outlet edges of runner blade at GHPS reveals that these have eroded over 40 years of operation and so replacement of existing runner blades with new manufactured one of improved profile and metallurgy is recommended.

6. ACKNOWLEDGEMENT

No financial aid were received for the project. The authors would like to express deepest appreciation to all faculty members of IOE Thapathali campus, Hydro lab Pvt. Ltd. (Lalitpur) and staffs of Gandak Hydropower Station for their continuous support, co-operation and guidance to complete the research .

REFERENCES

1. Bajracharya, T. R., Acharya, B., Joshi, C. B., Saini, R. P., & Dahlhaug, O. G. (2008). Sand erosion of Pelton turbine nozzles and buckets: A case study of Chilime Hydropower Plant. *Wear*, *264*(3–4), 177–184. https://doi.org/10.1016/j.wear.2007.02.021
2. Gupta, S. K., Prakash Maurya, A., Kumar Maurya, A., & Jhavar, P. (2017). DESIGN AND FLOW ANALYSIS OF ENHANCED KAPLAN TURBINE. *International Journal of Advance Research in Science and Engineering*, *06*(01).
3. Hari Prasad Neopane, B., Gunnar Dahlhaug, O., Cervantes, M., Prasad Neopane α, H., Gunnar Dahlhaug Ω, O., & Cervantes β, M. (2011). Sediment Erosion in Hydraulic Turbines. *Global Journal of Researches in Engineering Mechanical and Mechanics Engineering*, *11*(6).
4. Li, Y., & Liu, Q. (2020). Analysis of hydraulic performance for Kaplan turbine components based on CFD simulation. *IOP Conference Series: Earth and Environmental Science*, *510*(2). https://doi.org/10.1088/1755-1315/510/2/022038
5. NEA Generation Magazine, G. D. (2023). Generation Magazine 15th issue. *NEPAL ELECTRICITY AUTHORITY*. https://nea.org.np/admin/assets/uploads/annual_publications/Generation_2080.pdf
6. Neopane, H. P. (2010). *Sediment Erosion in Hydro turbines* [Norwegian University of Science and Technology]. http://hdl.handle.net/11250/233519
7. Poudel, L., Thapa, B., Shrestha, B. P., Shrestha, N. K., & Shrestha, B. P. (2012). Impact of Sand on Hydraulic Turbine Material: A Case Study of Roshi Khola, Nepal. *Hydro Nepal: Journal of Water, Energy & Environment*, *10*.
8. Prasad, R., & Rishideo, J. (2021). Sediment Load Concentration and Resultant Channel Planform in the Lower Gandak Plain. *International Journal of Research and Review*, *8*(12), 356–373. https://doi.org/10.52403/ijrr.20211244
9. RAI, A. K., & KUMAR, A. (2016). Analyzing hydro abrasive erosion in Kaplan turbine: A case study from India. *Journal of Hydrodynamics*, *28*(5), 863–872. https://doi.org/10.1016/S1001-6058(16)60687-X
10. Rajput, R. K. (2016). *A Textbook of Hydraulic Machines In SI Units* (R. . Rajput (ed.); Sixth Edit). S.CHAND & COMPANY PVT. LTD.
11. Sangal, S., Singhal, M. K., & Saini, R. P. (2016). CFD based analysis of silt erosion in Kaplan hydraulic turbine. *International Conference on Signal Processing, Communication, Power and Embedded System, SCOPES 2016 - Proceedings*, 1765–1770. https://doi.org/10.1109/SCOPES.2016.7955746
12. Shandilya, S., Shelar, S. P., Prasad Das, S., Chatterjee, D., & Saini, R. P. (2019). Performance evaluation of a bulb turbine designed for ultra-low head applications. *Journal of Physics: Conference Series*, *1276*(1). https://doi.org/10.1088/1742-6596/1276/1/012024
13. Thapa, B. (2004). *Sand Erosion in Hydraulic Machinery* [Norwegian University of Science and Technology (NTNU)]. http://hdl.handle.net/11250/231204
14. Thapa, B., Chaudhary, P., Dahlhaug, O. G., & Upadhyay, P. (2007). Study of Combined Effect of Sand Erosion and Cavitation in Hydraulic Turbines. *International Conference on Small Hydropower - Hydro Sri Lanka*, 22–24.
15. Thapa, B., Shrestha, R., Dhakal, P., & Thapa, B. S. (2005). Problems of Nepalese hydropower projects due to suspended sediments. *Aquatic Ecosystem Health and Management*, *8*(3), 251–257. https://doi.org/10.1080/14634980500218241
16. Versteeg, H. K., & Malalasekera, W. (2007). *An Introduction to Computational Fluid Dynamics* (Second). Pearson Education Limited. www.pearsoned.co.uk/versteeg
17. Weili, L., Jinling, L., Xingqi, L., & Yuan, L. (2010). Research on the cavitation characteristic of Kaplan turbine under sediment flow condition. *IOP Conference Series: Earth and Environmental Science*, *12*, 012022. https://doi.org/10.1088/1755-1315/12/1/012022